CAN UNCERTAINTY PROPAGATION SOLVE THE MYSTERIOUS CASE OF SNOOPY?

T. Caleb and S. Lizy-Destrez

ISAE-SUPAERO, 10 Avenue Edouard Belin, Toulouse, France, Email: {thomas.caleb@student., stephanie.lizy-destrez@}isae-supaero.fr

ABSTRACT

In 2015, a mysterious space debris entered the Earth's atmosphere under the name WT1190F. Even though it has been observed before, its origin remains an enigma. Two major candidates are considered: Snoopy, the lost lunar module of mission Apollo 10, launched in 1969, and the trans-lunar injection stage of Lunar Prospector, launched in 1998.

This study case raises the following question: How is it possible to compare 2 objects with their positions and uncertainties measured at different dates? This article will propose a probabilistic correlation criterion, able to compare the behaviour of two sets with one another. This criterion will then be evaluated on the case of WT1190F to determine which candidate is more likely to be the space debris.

Keywords: Uncertainty propagation; Snoopy case; WT1190F; Correlation criterion.

1. INTRODUCTION

Propagation of uncertainties is crucial in orbital mechanics, as every measurement of an orbit comes with an error. To that end, the impact of such errors must be quantified in order to estimate the position and velocity of the spacecraft with a given level of uncertainty. Thanks to these estimations, it is possible to approximate the collision probability of two objects, or the risk of failure of a rendezvous, for instance.

Several uncertainty propagation methods can be considered. Searching for a solution to the Fokker-Planck Equation can be done, it is a partial differential equation satisfied by the Probability Density Function (PDF), see [1]. This way, the PDF of the position of the spacecraft could be used easily. However, solving such an equation can be computationally expansive, especially for complex models due to heavy matrix computation.

It is the main reason why the work has been directed toward Monte-Carlo estimations, see [20]. Nevertheless, propagating a large number of trajectories can be very time-consuming and requires a lot of resources to parallelize computations. Therefore, Monte-Carlo estimations based on polynomial maps have been widely used over the past decades, particularly in orbital mechanics. Methodologies to perform faster Monte-Carlo estimations in without loss of accuracy, thanks to automatic domain splitting methods were proposed, see [4] and [24].

The main case study of this work is the space debris WT1190F, which entered the Earth's atmosphere in 2015, see [13]. It has been observed several times before, especially in 2013 under the name UDA34A3, see [12]. The origin of WT1190F is still a mystery, but studies tend to demonstrate that it is a man-made object returning to Earth. Among all the potential origins, see [8], can be found:

- Snoopy: the lost lunar module of mission Apollo 10 (LM-10), launched in 1969, see [2].
- LP-TLI: the trans-lunar injection stage of Lunar Prospector, launched in 1998, see [5, 3].

However, once the polynomial mapping of the uncertainty sets of WT1190F, LP-TLI and Snoopy is propagated to a common date, evaluating the correlation between WT1190F and Snoopy, and WT1190F and LP-TLI is a complicated task. Indeed, finding a single or a finite set of common points to the two sets has no weight compared to the infinite uncertainty sets. Moreover, it could be interesting to generate a large sample of each set and compute the distances between the samples. Yet, these distances would not take the shape of each uncertainty sets into account nor the probability to be in a part of a set of in another.

Thus, the need to find a way to compare the global behaviour of two uncertainty sets with one another in a probabilistic way. This article's aim is to display a methodology to do so in an efficient way.

This study will be structured into two parts. At first, the whole methodology to make such comparisons will be laid out, beginning with the description of the dynamics modelling, followed by the uncertainty propagation method, and by the construction of an *ad hoc* probabilistic correlation criterion, and the way to estimate it effi-

ciently. Then, this criterion will be computed to compare Snoopy and LP-TLI with respect to WT1190F.

2. BACKGROUND

The space debris WT1190F was observed several times, in 2013 under the names UDA34A3 or UW8551D. Another observation is sometimes linked to WT1190F: 9U01FF6 in 2009 and 2010. However, this link has not yet been established, due to close approaches with the Moon making the propagation difficult, see [12]. Furthermore, it is to be noted that data can be found on the physical parameters of UDA34A3, but not for WT1190F. It means that it is not possible to rely on observation to give WT1190F a mass or a surface for instance. Therefore, a hypothesis is needed to associate physical parameters to WT1190F. These parameters will only have an influence on the computation of the acceleration due to the Solar Radiation Pressure (SRP).

The object that is more likely to be WT1190F for [2] is Snoopy. The lunar module was jettisoned in a heliocentric orbit after the end its use by the crew of mission Apollo 10. The possibility of Snoopy's return was investigated for since 2018 at ISAE-SUPAERO, by F. Vagnone, L. Villanueva Rourera, P. Guardabasso and S. Lizy-Destrez, see [21, 23], and at CNES by D. Hautesserres, see [16]. Although no re-entry of Snoopy in the Earth's sphere of influence has ever been observed, Snoopy makes a close approach with Earth during the window of observation of WT1190F, see [9]. The initial state vector of Snoopy in 1969 is known as well as the physical parameters of Snoopy.

As for LP-TLI, its initial state vector of 1998 can be found in [5], and its physical parameters are available in [3]. However, no data is available regarding the uncertainties on the state vector, and the number of digits given in [5] is not enough to perform a thorough propagation of the uncertainty set until 2015.

Figure 1 illustrates the link between all objects, and the available data of their physical parameters. The two candidates are linked to WT1190F with dashed lines, while UDA34A3 is connected to it.

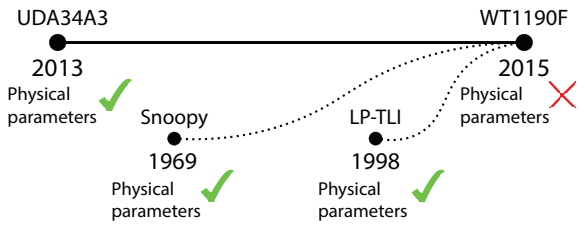

Figure 1. Summary of the data on the case studies

Furthermore, the propagation of the trajectory of these two objects from their initial epochs to 2015 to compare them with WT1190F is complicated, due to the accumulation of rounding errors, integration errors, and modelling errors. Even an accurate polynomial mapping of the uncertainty sets of the two would not deliver reliable results. Thus, the need to find another method to discriminate the two scenarios.

3. METHODOLOGY

The idea of this work is to use the fact that only the physical parameters of WT1190F are unknown, and then consider two scenarios:

1. WT1190F = Snoopy: Which consist in making the hypothesis that WT1190F has the same physical parameters as Snoopy
2. WT1190F = LP-TLI: Which consist in making the hypothesis that WT1190F has the same physical parameters as LP-TLI

Then, scenarios 1 and 2 will be compared to UDA34A3, used as a reference, with dynamics laid out in section 3.1, thanks to TDA propagations developed in section 3.2. Once the polynomial maps of each uncertainty sets is performed, the correlation criterion constructed in section 3.3 can be computed for each scenario with respect to UDA34A3 thanks to Monte-Carlo methods of section 3.5.

3.1. Dynamics

In this paper, the body under study will be called "spacecraft", even though this whole methodology can be applied to any object considered as a point mass.

The aim is to approximate the acceleration $\vec{\gamma}$ exerted on the spacecraft under study. This approximation will deliver an Ordinary Differential Equation (ODE) of order 2, linking the position $\vec{r}$ to the acceleration, thanks to Newton's second law:

$$\ddot{\vec{r}} = \vec{\gamma} \tag{1}$$

Solving this equation will provide the position and the velocity of the spacecraft.

The chosen dynamics model is based on ephemerides because of its high degree of accuracy compared to the N-body-problem, but with a higher computational cost. The library CSPICE provided by JPL, see [10], will be used to access the positions and velocities of the selected attracting bodies. The impact of the mass of the spacecraft is neglected on the trajectories of the celestial bodies. Furthermore, Solar Radiation Pressure (SRP) is the only perturbation taken into account, with a spherical model provided by R. M. Georgevic, see [11].

Thus, by using the Solar System barycenter as the origin and $J2000$ as the reference frame, the acceleration exerted on the spacecraft is:

$$\overrightarrow{\gamma} = \sum_{body \in bodies} \overrightarrow{\gamma}_{body} + \overrightarrow{\gamma}_{SRP} \tag{2}$$

With each gravitational acceleration generated by a celestial body computed independently in Cartesian coordinates as follows:

$$\overrightarrow{\gamma}_{body} = \mu_{body} \cdot \frac{\overrightarrow{r}_{body} - \overrightarrow{r}}{\left\| \overrightarrow{r}_{body} - \overrightarrow{r} \right\|^3} \tag{3}$$

With μ_{body} the mass parameter of a given body, and $\|\cdot\|$ the Euclidean norm. The Sun, all planets, Pluto and the Moon are taken into account to compute the acceleration.

And with SRP acceleration computed as follows:

$$\overrightarrow{\gamma}_{SRP} = -\frac{C_R S}{m} \cdot K_{SRP} \cdot \frac{\overrightarrow{r}_{Sun} - \overrightarrow{r}}{\left\| \overrightarrow{r}_{Sun} - \overrightarrow{r} \right\|^3} \tag{4}$$

With $K_{SRP} = 1.0227.10^{17}$ kg.m/s, m the spacecraft's mass, S the spacecraft's surface exposed to the SRP, and C_R the coefficient of reflexivity of the spacecraft, see [11]. The three last parameters are the only differences between the scenarios 1 and 2.

Then, the acceleration can be written as follows :

$$\overrightarrow{\gamma} = \sum_{body \in bodies} \overrightarrow{\gamma}_{body} \tag{5}$$

By changing the value of μ_{Sun} by :

$$\mu_{Sun} = \mu_{Sun} - K_{SRP} \cdot \frac{C_R S}{m} \tag{6}$$

Once the acceleration $\overrightarrow{\gamma}$ is modelled, the ODE 1 can be solved to know the position and velocity of the spacecraft.

3.2. TDA propagation

3.2.1. Implementing an TDA-compatible ODE solver

Form the perspective of TDA, considering f, a sufficiently regular function of v variables, or T_f, its Taylor expansion at order k is equivalent, see [6]. Algebraic operations $(+, -, \times, /)$ can be defined for the polynomials, as well as multiplication by scalars, derivation, integration, composition, $\sin$, $\exp$, etc... This set is a differential algebra of finite dimension equal to ${}_kD_v = \binom{k+v}{v}$. For this paper, the C++ library DACE, developed at Politecnico di Milano, was used to implement such a structure, see [19]. It can then be used to propagate a trajectory with a classic numerical integration algorithm. For instance, the propagation of the following Cauchy problem:

$$\begin{cases} \dot{y}(t) = f\left(y(t), t\right) \\ y(0) = y_0 \end{cases} \tag{7}$$

Then Euler's explicit method to approximate the solution of equation 7 is for a step h, for $n \in \mathbb{N}$, with $t_n = n \cdot h$, and with $y(t_n) = y_n$:

$$y_{n+1} = y_n + h \cdot f(y_n, t_n) + O(h^2) \tag{8}$$

If the measure of y_0 is tainted with errors, $[y_0]$, the class of equivalence of y_0 in ${}_kD_v$ is considered. It is a polynomial with its constant part equal to y_0 and with a non-constant part that represents the whole uncertainty space of y_0 up to the order n. Applying Euler's method (8) to $[y_0]$ delivers a Taylor expansion of the solution at each step, thanks to the algebra structure of ${}_kD_v$:

$$[y_{n+1}] = [y_n] + h \cdot f([y_n], t_n) + O(h^2) \tag{9}$$

The sequence $\left([y_n]\right)_{n \in \mathbb{N}}$ is a set of polynomials with the uncertainties on y_0 as variables. It represents the whole uncertainty set at each step t_n. Therefore, evaluating the impact of the initial uncertainties has a low computational cost since evaluating polynomials is cheaper than propagating a new set of initial conditions. The use of Euler's explicit method shows that any other ODE solver can be implemented following this method, since they only involve algebraic operations well-defined thanks to algebra structure.

In this paper, the algorithm DOP853 will be used to integrate the acceleration of equation 2, see [14]. This method is robust, of order 8, and has an adaptive step size.

Moreover, the approximation error due to the TDA approximation of the set is controlled thanks to an automatic domain splitting method, see [24]. The main idea behind this method is that the approximation error decreases exponentially with the size of the uncertainty set. Therefore, considering the uncertainty set as a collection of small sets instead of as large single one, considerably lowers the error at a cheap computational cost.

3.2.2. Modeling SRP uncertainties

Since the variables of the polynomials are used to evaluate the propagation of uncertainties, at least six variables are needed in order to capture uncertainties on the state vector. Moreover, uncertainties on the SRP are crucial in the case of long propagations, and they need to be modelled as well. To minimize computation time, all the uncertainties on SRP are represented by only one variable instead of three for S, C_R, and m:

$$[\overrightarrow{\gamma}_{SRP}] = K_{SRP} \cdot [C'_R] \cdot \frac{S}{m} \cdot \frac{\overrightarrow{r}}{r^3} \tag{10}$$

With:

$$\frac{\delta C'_R}{C'_R} = \sqrt{\left(\frac{\delta C_R}{C_R}\right)^2 + \left(\frac{\delta S}{S}\right)^2 + \left(\frac{\delta m}{m}\right)^2} \tag{11}$$

Since the dimension of ${}_kD_v$ is $\binom{k+v}{v}$, the dimension of the algebra modelling the uncertainties on the SRP for each source of error can be compared with the dimension of the simplified algebra with fewer variables. This ratio ${}_kr_v = \frac{{}_kD_v}{(k+2)D_v}$ is used to compare these two algebras:

$${}_kr_v = \frac{1}{\left(1+\frac{k}{v+1}\right)\left(1+\frac{k}{v+2}\right)} < 1 \tag{12}$$

Since $v = 7$ in this work :

Table 1. Value of ${}_nr_7$ for various TDA orders

k	${}_kr_7$
5	0.43
8	0.26
12	0.17
15	0.13

The ratio of the two dimensions in equation 12 captures the number of coefficients to be computed for each operation on an element of the TDA. In other words, it can be seen as the computation time ratio between the two algebras. From this point of view, and thanks to table 1, it is clear that modelling SRP uncertainties with only one variable is much more efficient. Furthermore, according to [22], the complexity of most operations in the TDA have a complexity higher than linear with respect to the dimension of the algebra. Therefore, the values of table 1 underestimate the gain provided by the expression of the SRP given by equations 10 and 11.

3.3. Correlation criterion

Now that uncertainty sets can be propagated thoroughly, how to express the similarity of two propagated sets? Let A and B be two spacecraft with given initial uncertainty sets $[x_A]$ and $[x_B]$ at given dates $t_A < t_B$. Is it possible to decide whether or not A and B are the same object?

3.3.1. Motivation : Why point-wise methods fail

Let T_A be a sample of the propagated uncertainty set of A from t_A to t_B. Can we conclude that A and B are the same if an element of T_A is included in $[x_B]$ at date t_B? Of course, it gives an hint of how A and B are related. But all it says in practice is that:

$$\exists S \subset T_A, S \subset [x_B] \tag{13}$$

But in that case S has a measure of zero. In other words, looking for the inclusions of points from a set in the other has no statistical meaning when infinite sets are considered.

The aim is to find a criterion that can translate the interaction of the two sets with one another.

3.3.2. Building a statistical criterion

Let $t \in [t_A, t_B]$, and $N \in \mathbb{N}$. Let T_A be a sample of size N of the propagated uncertainty set of A from t_A to t, and T_B be a sample of size N of the propagated uncertainty set of B propagated from t_B to t.

Let H_A be the convex hull of T_A, and H_B be the convex hull of T_B. In practice, H_A and H_B represent 6D volumes that envelop perfectly every element of T_A and T_B. This process is shown in figure 2. The approximation that H_A and H_B are the uncertainty sets at t of A and B is being made.

Then, the probability of the intersection of the two hulls represents the probability for each object to have a compatible state vector with the other and vice-versa. Because if A has the same state vector as B, then $A = B$. In other words, $P(H_A \cap H_B)$ is the probability for A and B to be the same object at a given date t.

However, this probability will be hard to estimate with Monte-Carlo methods expressed like that.

3.3.3. Finding a simple formula

Let $\Omega = T_A \cup T_B$ be the universe, and suppose that $Card(T_A) = Card(T_B) = N \in \mathbb{N}$. Since T_A are the points propagated from A, and T_B are the ones propagated from B, then:

$$T_A \cap T_B = \emptyset, \text{ and } T_A \cup T_B = \Omega \tag{14}$$

Then:

$$P(H_A \cap H_B) = P(H_A \cap H_B \cap T_A) + P(H_A \cap H_B \cap T_B) \tag{15}$$

Since $T_A \subset H_A$, and $T_B \subset H_B$:

$$P(H_A \cap H_B) = P(H_B \cap T_A) + P(H_A \cap T_B) \tag{16}$$

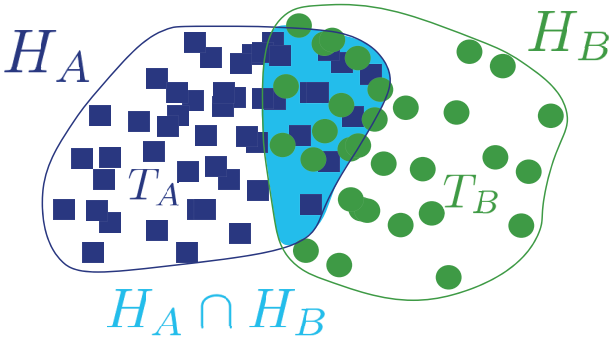

Figure 2. Correlation criterion principle

Then:

$$P\left(H_A \cap H_B\right) = P(T_A)P\left(H_B|T_A\right) + P(T_B)P\left(H_A|T_B\right) \tag{17}$$

Finally:

$$P\left(H_A \cap H_B\right) = \frac{1}{2}\left[P\left(H_B|T_A\right) + P\left(H_A|T_B\right)\right] \tag{18}$$

The correlation criterion is a function of t. It is the likelihood of the two objects to be the same. Moreover, it can be computed with Monte-Carlo methods. Being able to check inclusions of elements of T_A in H_B and vice-versa is the only requirement. This can be easily done, and confidence intervals can be computed on $P\left(H_B|T_A\right)$ and $P\left(H_A|T_B\right)$. Which means that a quantification of the error can also be performed on $P\left(H_A \cap H_B\right)$. This criterion can be easily generalized for any finite number of spacecraft, with the same method and properties.

3.4. Building hulls in practice

3.4.1. Drawbacks of *the* convex hull

The convex hull of a set is unique and there exist algorithms to build it. However, the convex hulls have several disadvantages:

- Complexity : The complexity of convex hull algorithms is exponential with respect to the dimension of the space, see [7]. Which makes it very hard to compute convex hulls for 10^5 points at hundreds of time steps.
- Storage : In six dimensions, the number of equations needed to represent all the surfaces of the hull grows rapidly, which can result in dozens of Gb of storage, which is already reserved for the storage of the polynomial maps.
- Checking inclusions : The formula of equation 18 shows that $2N$ inclusion checks are needed, and solving a linear system of such a size at each time step is not manageable.
- Methodology paradigm : The convex hull ensures that every building points will be included. However taking a point at a boundary and translating it of $10^{-13}AU$ away from the hull will deliver a point not included in it, even though propagation errors are beyond this magnitude. Therefore, this definition is not adapted to the whole methodology of this work. It should be possible to tune a tolerance parameter to adapt the swelling of the envelopes.

3.4.2. An alternative to *the* convex hull

A way to solve this problem is to use the Mahalanobis distance to build the hulls, see [18]. The idea is to perform a transformation from the Cartesian coordinate system to the coordinate system based on the mean of the cloud of points, with the eigenvectors of its covariance matrix has main directions. It means a unit is equal to a standard deviation in every direction. The computing of the euclidean distance in this transformed coordinate system is the Mahalanobis distance. The Mahalanobis distance with respect to a cloud of point $P \subset \mathbb{R}^6$ between two points $(x, y) \in \left(\mathbb{R}^6\right)^2$ is expressed in equation 19:

$$d_M(x, y) = \sqrt{(x-y)^T \Sigma^{-1} (x-y)} \tag{19}$$

With Σ the covariance martix of the cloud of points P.

The idea is to construct the hull of size α with the sphere in the Mahalanobis distance centered on the mean m, and of radius α. In other words, if $m \in \mathbb{R}^6$ is the mean of P, then the hull H of size α follows the expression of equation 20.

$$H = \left\{x \in \mathbb{R}^6, d_M(m, x) \leq \alpha\right\} \tag{20}$$

This has several advantages:

- Easy to compute: To build that hull, the only need is to estimate the mean of a $6D$ could of points, approximate its 6×6 covariance matrix, and invert it.

- Storage: Storing a Mahalanobis hull is equivalent to the storing 42 floating point digits per time steps, which is cheap.
- Check belongings: To check whether or not a point belongs to the hull, only a matrix-vector product and a scalar product need to be computed, which can be done efficiently.
- Paradigm: The Mahalanobis hulls offer a statistical solution to a statistical problem. The size of the hull can be increased or lowered as the user wishes. Furthermore, the size of the hull is not needed to build the hull. It is only necessary to check inclusions. Which makes it almost free to check inclusions in two hulls or more instead of in only one.

3.5. Monte-Carlo estimations

3.5.1. Generalities on Monte-Carlo estimations

Monte-Carlo methods are a way to estimate integrals with a statistical method, see [20]. The goal is to estimate an integral of the form of equation 21.

$$I = \int_{\mathbb{R}^d} \phi(x) f(x) dx \tag{21}$$

With f a density of probability, ϕ a given function, and $d \in \mathbb{N}$ the dimension of the problem.

The Monte-Carlo estimator of I is exposed in equation 22:

$$\hat{I} = \frac{1}{N} \sum_{i=1}^{N} \phi(X_i) \tag{22}$$

Where $N \in \mathbb{N}$ and the random variables in the sequence $(X_i)_{i \in \mathbb{N}}$ are independent and identically distributed random variables following the distribution f.

The law of large numbers ensures that $\hat{I} \longrightarrow E(\phi(X_1)) = I$ when $N \to \infty$, with $E(\cdot)$ the expectation.

3.5.2. Estimating the correlation criterion with Monte-Carlo

In this work, the random variables will be the state vectors of the spacecraft, mapped thanks to the TDA propagation. The main goal is to estimate each term of equation 18. The Monte-Carlo estimator $\hat{P}_{B|A}$ of $P\left(H_B|T_A\right)$ is given in equation 23, it is a similar estimator for $P\left(H_A|T_B\right)$.

$$\hat{P}_{B|A} = \frac{1}{N} \sum_{x_A \in T_A} \mathbb{1}_{H_B}(x_A) \tag{23}$$

Furthermore, it is possible to estimate the relative error made by the Monte-Carlo estimator, see [20]. Since $\mathbb{1}_{H_B}(x_A)$ follows a Bernoulli law of parameter $P\left(H_B|T_A\right)$, its variance is known and given in equation 24.

$$Var\left(\mathbb{1}_{H_B}(x_A)\right) = P\left(H_B|T_A\right) \cdot \left(1 - P\left(H_B|T_A\right)\right) \tag{24}$$

If $\Delta\hat{P}_{B|A} = 3.09 \cdot \frac{\sqrt{\hat{P}_{B|A} \cdot (1 - \hat{P}_{B|A})}}{\sqrt{N}}$, the Central Limit Theorem (CLT) delivers the expression of equation 25.

$$\left[\hat{P}_{B|A} - \Delta\hat{P}_{B|A}, \hat{P}_{B|A} + \Delta\hat{P}_{B|A}\right] \tag{25}$$

It is an estimation of the confidence interval at 99.9%, if $Var(P\left(H_B|T_A\right)) \neq 0$.

Furthermore, if $Var(P\left(H_B|T_A\right)) = 0$, thus, if $\hat{P}_{B|A} \in \{0, 1\}$, the confidence interval cannot by computed thanks to then CLT.

If $\hat{P}_{B|A} = 0$, the confidence interval at 99.9% is estimated thanks to [15], as in equation 26.

$$\hat{P}_{B|A} \in \left[0, \frac{6.9}{N}\right] \tag{26}$$

Symmetrically, if $\hat{P}_{B|A} = 1$, the confidence interval at 99.9% is estimated in the same way in equation 27.

$$\hat{P}_{B|A} \in \left[1 - \frac{6.9}{N}, 1\right] \tag{27}$$

Therefore, the equations 25, 26, and 27 offer a way to compute the error made on the estimation 23, based on the size of the sample N and on the estimation itself. It is now possible to estimate each term of the equation 18 and their confidence intervals. The size of the confidence interval $\Delta\hat{P}_{A \cap B}$ of $P\left(H_A \cap H_B\right)$, can be computed with equation 28, see [17].

$$\Delta\hat{P}_{A \cap B} = \frac{1}{2}\sqrt{\Delta\hat{P}_{A|B}{}^2 + \Delta\hat{P}_{B|A}{}^2} \tag{28}$$

The result of equation 28 can be easily generalized to any finite number of spacecraft too.

Finally, since $\hat{P}_{B|A} \cdot \left(1 - \hat{P}_{B|A}\right) \leq \frac{1}{4}$, the number of trajectories necessary to estimate the criterion with a given precision can bounded, thanks to equation 29.

$$\Delta\hat{P}_{B|A} \leq \frac{3.09}{2\sqrt{N}} \tag{29}$$

Therefore, equation 30 delivers the number of evaluation of the polynomial map needed.

$$\Delta\hat{P}_{A \cap B} \leq \frac{3.09}{2\sqrt{2N}} < \frac{1.1}{\sqrt{N}} \tag{30}$$

For instance, $N = 10^5 \implies \Delta\hat{P}_{A\cap B} < 3.5.10^{-3}$. Note that the result of equation 30 even works for the specific cases treated in equations 26 and 27, when $N > 20$, which is compulsory to perform a decent Monte-Carlo estimation.

4. RESULTS

The criterion of equation 18 is computed between WT1190F with the physical parameters of Snoopy and UDA34A3 (scenario 1), and also for WT1190F with the physical parameters of LP-TLI and UDA34A3 (scenario 2). The aim is to compare the two scenarios exposed in section 3. The criteria are computed for 6 months in 2013 to let time to the two scenarios to diverge from one another. The chosen size of the hulls is $\alpha = 5000$. The result is plotted in figure 3, with the normalized distance from UDA34A3 to Earth plotted in cyan dashed lines as reference.

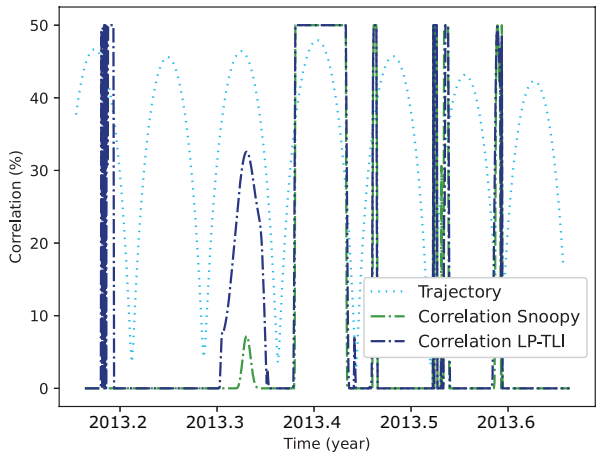

Figure 3. Correlation criteria of the two scenarios

It appears in figure 3 that LP-TLI is more likely to be UDA34A3 than Snoopy at several dates. But this conclusion is not clear yet. Furthermore, it is possible that the size of the hulls α changes the behaviour of the criteria. It is the reason why each curve is integrated during this window for $\alpha \in [0, 5000]$ in figure 4.

Figure 4 highlights the fact that for any hull size, the scenario LP-TLI = WT1190F (scenario 2) is always more likely, with a 31% advantage when $\alpha = 5000$.

Regarding the performances, the whole study was performed in 5 h, including the TDA propagations of UDA34A3, and the two versions of WT1190F. These three propagations were realized simultaneously, and make up for the major part of the 5 h. The evaluation of polynomial maps, the construction of the hulls, and the inclusion checks can be neglected as they represent less than 4% of the total computational time. The sample size is of 10^5, which makes the average computation time of

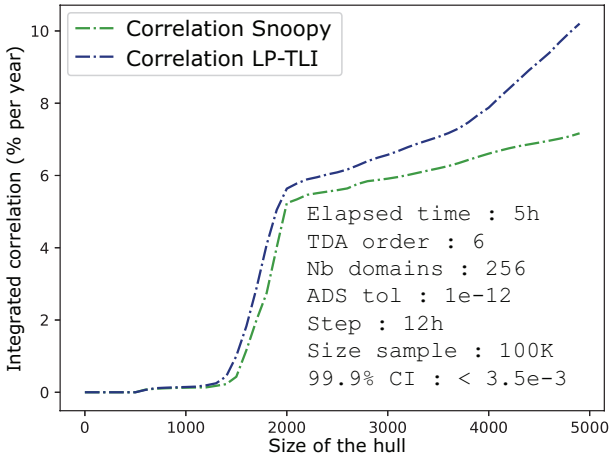

Figure 4. Integrated correlation criteria of the two scenarios

a single floating point trajectory 0.18 s, which is a convincing performance for a propagation of 2 years with a step of 12 h.

5. CONCLUSION AND FUTURE WORK

This article proposes a way to quantify the interactions of two uncertainty sets propagated from different dates with one another. The proposed criterion to do so is probabilistic and translates the behaviour of the two sets in their entirety, without making point-wise comparisons. It can be easily evaluated with Monte-Carlo methods, providing confidence intervals. And the computation time of such a criterion can be neglected compared to the propagations of the uncertainty sets. Moreover, this criterion offers a tolerance parameter to tune the size of the hulls.

This criterion was then applied to the case study of Snoopy and the trans-lunar injection stage of Lunar Prospector (LP-TLI), to determine which one is more likely to be the space debris WT1190F. Results show that LP-TLI is more likely to have reentered in the Earth's atmosphere under the name WT1190F, with a 31% advantage. Therefore, Snoopy is still likely to be orbiting the Sun. Even though it provides a good hint on where to focus the research, such a result does not allow to make a clear conclusion on the origin of the space debris. Nevertheless, it is to be noted that the Solar Radiation Pressure (SRP) is the only responsible for the differences between the two scenarios, which can explain such a small variability between the two.

Regarding the case of WT1190F, future work will be dedicated to refining the spherical modelling of the SRP, considering the impact of this force in this study. Dynamical models could be introduced, taking into account the variations in the power radiated by the Sun for instance. Moreover, it could prove interesting to implement the drag due to the Earth's atmosphere. Indeed, this force

differs from one scenario to the other, and will probably lead to an even greater difference.

Regarding the criterion itself, it could prove interesting to give a more precise meaning to the size of the hull α from a probabilistic point of view. Such a knowledge would make the setting of this parameter easier. Furthermore, building a bank of test cases of comets, asteroids, and man-made spacecraft would allow to have more data on the behaviour of this criterion on known study cases. The efficiency of the criterion in various situations could then be evaluated, before applying it to ongoing investigations.

ACKNOWLEDGMENTS

The authors would like to thank Denis Hautesserres (CNES) for his expertise in numerical analysis, numerical integration, and for the very interesting discussions on the case of Snoopy. Also, Roberto Armellin and Laura Pirovano (University of Auckland) for providing the automatic domain splitting algorithms. Moreover, the authors would like to thank Federica Vagnone, Lydia Villanueva Rourera and Paolo Guardabasso (ISAE-SUPAERO) for their work on the trajectory of Snoopy.

REFERENCES

1. ACCIARINI, G., GRECOY, C., AND VASILE, M. On the solution of the fokker-planck equationwithout diffusion for uncertainty propagation inorbital dynamics.
2. ADAMO, D. R. Earth departure trajectory reconstruction of apollo program components undergoing disposal in interplanetary space. *http://www.aiaahouston.org* (2012).
3. ANDOLZ, F. J. Lunar prospector mission handbook. Tech. rep., Lockheed Martin Missiles and Space Co., 1998.
4. ARMELLIN, R., DI LIZIA, P., BERNELLI-ZAZZERA, F., AND BERZ, M. Asteroid close encounters characterization using differential algebra: The case of apophis. *Springer* (2010).
5. BECKMAN, D., AND FOLTA, M. Lunar prospector mission design and trajectory support. In *AAS SFD* (1998).
6. BERZ, M. *Modern Map Methods in Particle Beam Physics*. Academic Press, 1999.
7. BRADFORD BARBER, C., DABKIN, D., AND HUHDANPAA, H. The quickhull algorithm for convex hulls. *ACM Transactions on Mathematical Software* (1996).
8. BUZZONI, A., ALTAVILLA, G., FAN, S., FRUEH, C., FOPPIANI, I., MICHELI, M., NOMEN, J., AND SANCHEZ-ORTIZ, N. Physical characterization of the deep-space debris wt1190f: Atestbed for advanced ssa techniques. *Advances in Space Research* (2018).
9. CALEB, T., AND LIZY-DESTREZ, S. Can uncertainty propagation solve the mysterious case of snoopy? *UQOP2020* (2020).
10. FOLKNER, W. M., WILLIAMS, J. G., BOGGS, D. H., PARK, R. S., AND KUCHYNKA, P. The planetary and lunar ephemerides de430 and de431. Tech. rep., Jet Propulsion Laboratory, California Institute of Technology, 2014.
11. GEORGEVIC, R. M. Mathematical model of the solar radiation forceand torques acting on the componentsof a spacecraft. Tech. rep., Jet Propulsion Laboratory, 1971.
12. GRAY, B. "pseudo-mpec" for uda34a3 = uw8551d. https://www.projectpluto.com/pluto/mpecs/uda.htm, 2014.
13. GRAY, B. "pseudo-mpec" for uda34a3 = uw8551d = wt1190f. https://projectpluto.com/temp/mpec9.htm#r001, 2015.
14. HAIRER, E., NØRSETT, S. P., AND WANNER, G. *Solving Ordinary Differential Equations I Nonstiff Problems*. Springer, 1993.
15. HANLEY, J A LIPPMAN-HAND, A. If nothing goes wrong, is everything all right? interpreting zero numerators. *Journal of the American Medical Association* (1983).
16. HAUTESSERRES, D., VILLANUEVA ROURERA, L., AND GUARDABASSO, P. Research of the history of wt1190f and that of snoopy. Tech. rep., Centre National d'Etudes Spatiales (CNES) and Institut Supérieur de l'Aéronautique et de l'Espace (ISAE-SUPAERO), 2020.
17. KOKOSKA, S., AND NEVISON, C. *Statistical Tablesand Formulae*. Springer-Verlag, 1989.
18. MAESSCHALCK, R. D., JOUAN-RIMBAUD, D., AND MASSART, D. L. The mahalanobis distance. *Chemometrics and Intelligent Laboratory Systems* (2000).
19. MASSARI, M., DI LIZIA, P., AND RASOTTO, M. Nonlinear uncertainty propagation in astrodynamics using differential algebra and graphics processing units. *American Institute of Aeronautics and Astronautics* (2017).
20. ROBERT, C. P., AND CASELLA, G. *Monte Carlo Statistical Methods*. Springer, 2004.
21. VAGNONE, F. Snoopy's trajectory – debris identification. Tech. rep., ISAE-SUPAERO, 2018.
22. VASILE, M., ORTEGA ABSIL, C., AND RICCARDI, A. Set propagation in dynamical systems with generalised polynomial algebra and its computational complexity. *Commun. Nonlinear Sci. Numer. Simul.* (2019).
23. VILLANUEVA ROURERA, L., LIZY-DESTREZ, S., AND GUARDABASSO, P. Snoopy's trajectory - debris identification. Tech. rep., Institut Supérieur de l'Aéronautique et de l'Espace (ISAE-SUPAERO), 2020.

24. WITTIG, A., DI LIZIA, P., ARMELLIN, R., MAKINO, K., BERNELLI-ZAZZERA, F., AND BERZ, M. Propagation of large uncertainty sets in orbital dynamics by automatic domain splitting. *Springer, Celest Mech Dyn Astr* (2015).